HHS Public Access

Author manuscript

J Neuropsychiatry Clin Neurosci. Author manuscript; available in PMC 2021 December 30.

Published in final edited form as:

J Neuropsychiatry Clin Neurosci. 2020 ; 32(4): 352–361. doi:10.1176/appi.neuropsych.19100221.

Comparison of T1rho MRI, Glucose Metabolism and Amyloid Burden Across the Cognitive Spectrum: Pilot Study[1]

Laura L. Boles Ponto, Ph.D.[a], **Vincent A. Magnotta, Ph.D.**[a,b], **Yusuf Menda, M.D.**[a], **David J. Moser, Ph.D.**[b], **Jacob J. Oleson, Ph.D.**[c], **Emily L. Harlynn, B.S.**[a], **Sean D. DeVries, M.S.**[c], **John A. Wemmie, M.D., Ph.D.**[b], **Susan K. Schultz, M.D.**[b]

[a]Department of Radiology, Carver College of Medicine, University of Iowa

[b]Department of Psychiatry, Carver College of Medicine, University of Iowa

[c]Department of Biostatistics, College of Public Health, University of Iowa

Abstract

The pathological cascades associated with the development of Alzheimer's disease (AD) - amyloid pathology, tau pathology, vascular insufficiency, metabolic disturbances and oxidative stress – have a common element – acidosis. T1rho (spin lattice relaxation time in the rotating frame) MRI is a pH sensitive measure with higher values associated with greater neuropathological burden.

Methods—Twenty-seven participants (13M,14F, 55 – 90 years) across the cognitive spectrum (17 healthy controls (HC), 7 mild cognitive impairment (MCI), 3 mild Alzheimer's disease (AD)) underwent neuropsychological testing, MR imaging (T1-weighted and T1rho (spin lattice relaxation time in the rotating frame)) and PET imaging ([^{11}C]PIB for amyloid burden (N=26), and [^{18}F]fluorodeoxyglucose for cerebral glucose metabolism (N=12)). The relationships between global T1rho values and the neuropsychological, demographic and imaging measures were explored.

Results—Global mean and median T1rho were positively associated with age. After controlling for age, higher global T1rho was associated with poorer cognitive function, poorer memory function (immediate and delayed memory scores)), higher amyloid burden, and more abnormal cerebral glucose metabolism. Regional T1rho values, when controlled for age, significantly differed between cognitively normal and impaired groups for select frontal, cingulate and parietal regions.

Conclusion—Higher T1rho values were associated with greater cognitive impairment and pathological burden. T1rho, a biomarker that varies according to a feature common to each of

---

[1]A portion of this work has previously been presented in abstract form at the following meetings:
Ponto LL, Schultz SK, Jacob M, Menda Y, Wemmie J, Magnotta VA. Brain pH and Alzheimer's Disease. SNMMI Annual Meeting 2014, St. Louis, Missouri. June 7 – 11, 2014, # 192. Journal of Nuclear Medicine, 2014 (May); 55(Supplement 1): 192.
Ponto LLB, Schultz SK, Menda Y, Arndt S, Magnotta VA. Alzheimer's pathology and the pH-sensitive marker T1rho MRI. SNMMI Annual Meeting 2016, San Diego, California, June 11 – 15, 2016, abstract #129, Monday, June 13, 2016. Journal of Nuclear Medicine. 2016; 57(Suppl 2): 67P. http://edition.pagesuite-professional.co.uk/launch.aspx?eid=6104d3d1–717b-4ddd-a317-b29a5d29272f

Corresponding author: Laura L. Boles Ponto, Ph.D., Professor, PET Imaging Center, University of Iowa Hospitals and Clinics, 200 Hawkins Drive, Iowa City, Iowa 52242, laura-ponto@uiowa.edu, 319-356-1857 (tel), 319-353-6512 (fax).

the cascades rather than one unique to a particular pathology, has the potential to serve as a metric of neuropathology theoretically providing a measure for assessing pathological status and for monitoring the trajectory of neurodegeneration over time.

Introduction

The pathophysiology of Alzheimer's disease (AD) has been characterized as multifactorial processes that lead to the death of cholinergic neurons and eventually the clinical symptoms of AD. Humpel{1} has proposed a "common unifying hypothesis" that combines the vasculopathy (i.e., impaired blood flow) and β-amyloid cascade hypotheses to explain how amyloid pathology, tau pathology, vascular insufficiency, metabolic disturbances and oxidative stress all, jointly or individually, can lead to cell death. An alternative explanation is posed by the mitochondrial cascade hypothesis{2}. This hypothesis proposes that mitochondrial function declines until bioenergetic failure occurs. This failure precipitates β-amyloid production and subsequent plaque deposition, as well as tau phosphorylation leading to tangle formation, and synaptic loss with subsequent neurodegeneration.{3}

A common element in each of these pathological cascade hypotheses is the presence of acidosis. Acidosis is the result of increased levels of CO_2 or accumulation of acidic by-products of dysfunctional metabolism. Acidosis may represent both an early sign of mitochondrial dysfunction as well as a facilitator of the pathological process itself by enhancing β-amyloid aggregation, production of reactive oxygen species (ROS){4}, and cholinergic cell death.{1}

Brain imaging techniques are currently available for the assessment of many of the branches of the pathological cascade including vascular insufficiency (cerebral blood flow imaging ([^{15}O]water), arterial spin labeling (ASL)), glucose metabolic disturbances ([^{18}F]fluorodeoxyglucose (FDG)), β-amyloid clearance and plaques (amyloid imaging agents (e.g., [^{18}F]florbetapir, [^{18}F]florbetaben, [^{18}F]flutemetamol, [^{11}C]PIB), tau pathology (e.g., [^{18}F]flortaucipir), and cell death with associated atrophy (structural MRI). However, each technique examines a specific component of AD-associated pathology in isolation. None of these techniques supplies a composite picture of the status of the individual on the dementia pathological trajectory, yet, each pathology contributes to the cognitive deterioration. Imaging measures that vary with the overall burden or that assesses a common feature (e.g., acidosis) of pathologies that impact neuropsychological function may represent a means of compositing all of these pathological processes into a single metric.

A number of prior studies{5–10} have shown that T1rho MRI (spin lattice relaxation in the rotating frame) is sensitive to pH. A consistent finding in these prior studies was that higher T1rho relaxation times corresponded to a lower pH (higher T1rho = lower pH = more acidic). This relationship held across a wide range of magnetic field strengths (3.0–9.4T) and spin-lock amplitudes (2.9–94μT). Furthermore, work by Owusu et al has found that the strongest contribution to changes appear to be pH at 3T using spin-lock amplitudes that can be achieved with FDA limits of subject heating.{11} Work by Magnotta, et al.{7, 12–14} has evaluated the use of T1rho MRI to examine brain pH and has explored the potential utility of this technique in distinguishing the pathologies underlying panic disorder{15},

bipolar disorder{16, 17} and premanifest Huntington's disease (HD){18}. In each disorder, the T1rho signal was elevated in specific regions known to be adversely affected in the particular disease in the patients with the neuropsychiatric disorder compared to control subjects (e.g., striatum in HD{18}).

Work in Alzheimer's disease (AD){19–23} has reported differences in the T1rho signal that may distinguish healthy controls from individuals with cognitive impairment (mild cognitive impairment (MCI) and AD). The T1rho signal in the temporal lobe alone{20, 22} and in combination with CSF biomarkers{23} distinguished the groups. Furthermore, the T1rho signal in the hippocampus{21} was potentially useful in distinguishing AD from Parkinson's disease without (PD){24} and with associated dementia (PDD).{21, 25} In addition, the T1rho signal in the substantia nigra was correlated with the asymmetry of PD motor symptoms (UPDRS scores).{25}

The AD-related research with T1rho has focused on the medial temporal lobe structures and, except for the work of Haris, et al.{23}, depended solely on subject classification based on neuropsychological/clinical evaluations. None of the dementia-related investigations examined the T1rho signal, both globally and regionally, compared to imaging-based measures of the AD-associated pathological processes (e.g. amyloid, glucose hypometabolism).

The purpose of this research was to investigate the relationship between T1rho imaging and AD-associated pathologies as determined by available diagnostic imaging techniques. The techniques employed utilized measures of brain metabolism, specifically glucose metabolism with [^{18}F]fluorodeoxyglucose (FDG), and AD-associated pathology, specifically, amyloid burden with [^{11}C]PIB PET imaging. It was hypothesized that higher T1rho signal would be associated with more abnormal function or greater pathological burden, specifically, lower FDG uptake, greater AD-associated pathology (i.e., amyloid burden), and poorer cognitive performance. Age was considered as a potentially important covariate in the analyses because of the conflicting findings in regard to the association between T1rho and age. Zhao, et al.{26} has observed significant increases in T1rho signal associated with age-related changes in the rat brain. These findings are consistent with the work of Menyhart, et al.{27} who found tissue acidosis in the aged rat brain, due to alterations in the pH-shift induced from spreading depolarization (SD). It was hypothesized that the SD-induced acidic pH shift was the result of a persistent elevation in the lactate concentration due to reductions in the facilitated diffusion of lactate into the bloodstream in the aged brain. In human studies, some authors have found no relationship between T1rho and age{21–23} or non-statistically significant increases in the T1rho signal with age{20} when examining limited areas of the brain (e.g., medial temporal lobe, hippocampus). However, Watts, et al.,{28} found significant decreases in cortical gray matter, caudate, putamen, hippocampus, amygdala and nucleus accumbens, but significant increases with age in white matter tracts. Recent *in vitro* work in human neocortical tissues resected from patients undergoing epilepsy surgery found a mild acidification with age.{29} It was hypothesized that the age-related decrease in neuronal intracellular pH might be associated with beneficial neuroprotection by limiting excitotoxicity. On the other hand, intracellular

acidification can induce apoptosis and promote the development of Alzheimer's dementia. {30} Therefore, age was considered in all analyses.

Materials and Methods

Participants

Male and post-menopausal female participants, age 55 – 90 years, who were cognitively healthy, had mild cognitive impairment (MCI) or early Alzheimer's disease (AD) based on clinical criteria were eligible for inclusion. Participants were excluded if they were unable to undergo MR imaging, had a history of or current diagnosis of major psychiatric disease (other than dementia), a history of abuse of psychoactive substances or medications, a history of stroke, a history of head injury with loss of consciousness for greater than 30 minutes, or a history of other neurological disorder or systemic illness that could potentially affect cognition or brain function (outside of a diagnosis of AD or MCI) or could affect their safety or comfort while undergoing the imaging studies. The study was approved by the University of Iowa Institutional Review Board and Medical Radiation Protection Committee and all participants signed a written informed consent form. Participants were placed into cognitive classifications based on methods validated by the Alzheimer's Disease Neuroimaging Initiative{31} or if they had already undergone a comprehensive clinical evaluation with confirmation of the diagnosis through longitudinal follow-up, then their current clinical diagnosis was used.

PET Radiopharmaceuticals

[^{11}C]PIB was prepared according to the methods and met all specifications detailed in the CMC section of the University of Iowa's IND application, #109,386, Michael M. Graham, M.D. (physician-sponsor). [^{18}F]Fluorodeoxyglucose (FDG) was produced according to the University of Iowa's ANDA.

Imaging:

All participants underwent MR imaging including T1rho imaging, neuropsychological testing and [^{11}C]PIB PET imaging. A subset of participants also underwent FDG imaging for assessment of cerebral glucose metabolism. All PET imaging was performed on a Siemens ECAT EXACT HR+ with transmission imaging ([^{68}Ge]) for attenuation correction performed prior to the injection of the radiotracers. MR imaging was performed on a 3.0T Siemens TIM Trio MRI Scanner. All image analyses were performed using the PMOD suite of tools (PVIEW, PFUSION, PNEURO, PXMOD, PKIN, PALZ, v. 3.7 and 3.8, PMOD Technologies, Ltd, Zurich, Switzerland).

[^{18}F]Fluorodeoxyglucose (FDG)

Participants fasted for a minimum of 6 hours prior to the FDG administration. The blood glucose level was checked prior to FDG administration and in all cases was ≤ 200 mg/dL (range 70 – 188 mg/dL). FDG (185 MBq ± 10% (5 mCi ± 10%) IV) was administered and imaged dynamically for 60 minutes. The scanner was in a quiet, darkened room and the participant had their eyes open and ears unplugged during the uptake and imaging period. Dynamic data were iteratively reconstructed (Gaussian 3.0, 6 iterations/16 subsets, zoom =

2.6, attenuation, scatter, decay and deadtime correction = ON) and summed from 30 to 60 minutes.

[^{11}C]PIB Imaging

Participants were injected with [^{11}C]PIB (555 MBq ± 10% (15 mCi ± 10%) IV) on the scanner and imaged dynamically for 90 minutes. The ambient conditions during imaging were similar to that experienced during the FDG condition. Dynamic data were iteratively reconstructed (Gaussian 3.0, 6 iterations/16 subsets, zoom = 2.6, attenuation, scatter, decay and deadtime correction = ON) and a summed image was created with the data from 50 to 70 minutes post-administration.

MR Imaging

A multi-modal MRI protocol was collected that included: 1) 3D high resolution anatomical images (T1 – 3D MP-RAGE and T2 – 3D SPACE); and 2) volumetric T1rho images (3D FLASH: TE=3.5ms, TR=7.6ms, flip angle = 15°, FOV=240×240×100, Matrix=128×128×20, Bandwidth=260Hz/pixel, B_1 amplitude=250Hz, spin-lock times = 10, 60ms).{32} The T1rho data were conducted during rest in order to parallel the [^{11}C]PIB and FDG conditions.

Image Analysis

General—Activity and parametric PET images were co-registered to the individual's T1-weighted anatomical MRI using the FUSION tool of PMOD. MRI-based volumes-of-interest (VOIs) were determined on the T1-weighted MRI using the maximum probability atlas and the brain parcellation tools of the NEURO tool of PMOD. The VOIs were transferred to the co-registered PET and T1rho images. Measures from these VOIs (as implemented by the NEURO tool of PMOD) were used for comparative analyses. Individual cortical volumes were calculated by summing the left and right hemispheric cortical volumes as determined by the brain parcellation tool.

FDG Processing—The FDG data were summed from t = 30 to 60 minutes and converted to SUV units. FDG images were analyzed by volume-of-interest (VOI) based on the individual's structural MRI as well as using a software tool designed specifically for the analysis of FDG images and assessing the risk of AD (Alzheimers Discrimination Tool (PALZ) PMOD Technologies, LTD)).

[^{11}C]PIB Imaging—Amyloid burden was determined using methods described by Price, et al.{33} and Lopresti, et al.{34} The distribution volume ratio (DVR) was calculated for each region based on the fit employing the simplified reference tissue method 2 (SRTM2) as implemented by the kinetic tool (PMOD PKIN) using the nonspecific retention in the reference region (in this case, bilateral cerebellar gray matter) and the 90 minutes of data. In addition, the simple standardized uptake value ratios (SUVRs) were calculated for each region using the SUV for the interval from 50 to 70 minutes post-administration and the bilateral cerebellar gray matter as the reference tissue.

The primary outcome variable from the [^{11}C]PIB component of the study was the composite measure of amyloid burden (based on the volume-weighted mean of frontal, parietal, lateral temporal, anterior and posterior cingulate regions), referred to as a cortical retention ratio (CRR), and regional measures of amyloid burden derived from DVR and SUVR values. These values each had corresponding global and regional measures of glucose metabolism (i.e., FDG SUV) and the MRI-based T1rho values (global and regional mean and median T1rho values).

T1rho MRI Processing

The volumetric T1rho images were acquired using a coronal 3D FLASH sequence as described above. The T1rho relaxation times were calculated by fitting the voxel intensities versus the spin-lock time using a mono-exponential signal decay model. The resulting images were co-registered with the T1-weighted anatomical images and the VOIs were defined as previously described. For each region, the mean and the median values were available. Because of the potential of CSF spillover unduly influencing the mean value, the median value for each region was also investigated. The global T1rho mean and median values were calculated by calculating a volume-weighted average of the T1rho values for all intracerebral pixels as determined from the co-registered structural MRI. Because of the potential for incomplete coverage of the entire brain with the MRI field-of-view, regional comparisons and global calculations were limited to regions that had a minimum pixel value > 0.

Consideration of Age

Age was considered as a potentially important covariate in the analyses because of the conflicting findings in regard to the association between T1rho and age. Zhao, et al.{26} has observed significant increases in T1rho signal associated with age-related changes in the rat brain. These findings are consistent with the work of Menyhart, et al.{27} who found tissue acidosis in the aged rat brain, due to alterations in the pH-shift induced from spreading depolarization (SD). It was hypothesized that the SD-induced acidic pH shift was the result of a persistent elevation in the lactate concentration due to reductions in the facilitated diffusion of lactate into the bloodstream in the aged brain. In human studies, some authors have found no relationship between T1rho and age{21–23} or non-statistically significant increases in the T1rho signal with age{20} when examining limited areas of the brain (e.g., medial temporal lobe, hippocampus). However, Watts, et al.,{28} found significant decreases in cortical gray matter, caudate, putamen, hippocampus, amygdala and nucleus accumbens, but significant increases with age in white matter tracts. Recent *in vitro* work in human neocortical tissues resected from patients undergoing epilepsy surgery found a mild acidification with age.{29} It was hypothesized that the age-related decrease in neuronal intracellular pH might be associated with beneficial neuroprotection by limiting excitotoxicity. On the other hand, intracellular acidification can induce apoptosis and promote the development of Alzheimer's dementia.{30} Therefore, age was considered in all analyses.

Statistical Analyses

The outcome variables of interest were the Global Mean T1rho and the Global Median T1rho scores. Using linear regression models, the relationships of age with both outcome variables were evaluated followed by evaluations of the relationships between the imaging-based variables with T1rho, both mean and median, after adjusting for age. None of the variables had a significant interaction with age, so only main effects are reported. The R^2 is reported for each model as well as the increase in R^2 over the age only model. Then, to assess which regions of the brain showed relationships between T1rho measures (mean and median) and cognitive status (i.e., cognitively normal = HC or cognitively abnormal = MCI_AD) controlling for age, separate regression models for each region were run. To adjust for the evaluation of multiple models, the p-values were adjusted using the False Discover Rate (FDR{35}). Analyses were carried out using SAS/STAT software v 9.4.

Results

Subject Demographics

Twenty-seven community-dwelling participants, 13 males, 14 females with a mean age = 71.8 ± 11.3 years (range: 55 – 90 years), were studied. Cognitively, 17 participants were classified as healthy controls (HC), 7 as mild cognitive impairment (MCI, 6 early (eMCI) and 1 late-stage (lMCI)), and 3 as suffering from mild Alzheimer's disease (AD) resulting in 10 subjects with cognitive impairment. Complete data were available for 11/12 participants with FDG imaging. One AD participant was unable to undergo the PIB imaging component due to his moving away from the study locale. His data were included in the analyses when available. The AD and lMCI participants were all males. In the FDG cohort, the lMCI was the only subject with Type II diabetes. Demographic, neuropsychological and global image-based measures are presented in Table 1.

Relationships between T1rho and Global Measures

The relationship between the global mean and global median T1rho values and neuropsychological and functional/pathological variables are presented in Table 2. Age was a highly significant predictor of the global mean and median T1rho values, accounting for > 30 % of the variance. Therefore, age was factored in the balance of the comparisons. With age in the model, the addition of other relevant AD-associated parameters, improved the explanation of the variance in T1rho by 17 to 42%. Higher T1rho values were associated with a clinical diagnosis of cognitive impairment (i.e.,MCI or AD diagnosis), poorer neuropsychological test performance (i.e., lower MMSE, poorer logical memory (both immediate and delayed), longer times to complete the Trailmaking Test B-A), more abnormal glucose metabolism (i.e., higher Alzheimer's discrimination score (PALZ)) and higher amyloid burden (i.e., cortical retention ratio based on distribution volume ratio (DVR) or standardized uptake volume ratio (SUVR)).

Figure 2 presents these relationships graphically in the form of contour plots of the relationship between T1rho and selected pathological measures color-coded by MMSE. Note the increased T1rho values with greater pathological burden and associated poorer cognition (i.e., MMSE: red<gray<blue). Increasing age (far right contours) did not exhibit

the progressive decline in MMSE that was observed with increasing pathologies (CRR (far left) or PALZ score) (middle contours)).

Cortical volume, as a surrogate for neurodegeneration, was significantly related to age ($r = -0.67$, $p = 0.0001$). and to the T1rho measures (mean: $r = -0.63$, $p = 0.0005$; median: $r = -0.63$, $p = 0.0004$). With age and T1rho in the model, cortical volume was not significantly related to any of the neuropsychological or pathological measures with p-values ranging from $p = 0.13$ to 0.77. Therefore, T1rho is a stronger predictor than cortical volume for AD-associated neuropsychiatric measures.

Relationships between T1rho and Regional Measures

The relationship between regional T1rho measures (mean and median) and cognitive status controlled for age is presented in Table 3. Of the 78 available regions for analysis, the regions reported are limited to those for which both age and the status variable were statistically significant. The bolded regions are those for which the cognitive status p-value remained significant after the false discovery rate (FDR) correction. In all cases, the healthy control participants (HC) exhibited a lower T1rho value than the cognitively-impaired participants. Note that except for the bilateral thalami and the right insula (which are no longer statistically significant after the false discovery rate (FDR) correction), all significant regions are located in the frontal, cingulate, temporal or parietal lobes, areas known to have significant amyloid deposition and to be selectively metabolically compromised in Alzheimer's disease.

Discussion

At present, there are no disease-modifying therapies available for Alzheimer's disease. More and more evidence points to the necessity of treating AD in the presymptomatic stage rather than waiting for the advent of a specific threshold initiation of a pathological cascade. However, the ability to diagnose AD depends on diagnostic tests performed in isolation, and, for a given level of cognitive impairment, the biomarker profile can be markedly different between individuals.{36} An *in vivo* measure that characterizes the brain microenvironment and/or pathological burden such as T1rho has the potential to provide a means to place an individual on the pathological continuum and to follow the trajectory over time better than single function or pathology-oriented measures. Furthermore, this measure can be used serially without concern for the accumulated radiation burden associated with FDG, amyloid and/or tau imaging.

T1rho increases with age and with increasing AD-associated pathologies. This observation is consistent with the reported relationship between age on brain pH. Bonnet, et al.,{29} reported a correlation between age and pH in the middle temporal gyrus of $r = -0.68$. In the current investigation, the correlation between age and T1rho (inversely related to pH) was $r = 0.57$ and $r = 0.53$ in the left and right superior posterior temporal gyrus, respectively, and 0.88 and 0.82 in the left and right posterior temporal lobe, respectively. Therefore, the relationship between age and a surrogate for pH, i.e., T1rho, was comparable to the direct relationship observed between age and pH. Beyond that relationship and consistent with the role of acidosis in the pathological cascades, after controlling for age, T1rho increases with

impaired cognition (decreasing MMSE, poorer immediate and long-term memory scores), increasing amyloid burden (based on PIB-based cortical retention ratios), and more aberrant glucose metabolism (based on FDG-based metabolism).

Previous work exploring the potential utility of T1rho imaging in AD has exhibited promising results but has suffered from limitations regarding the extent of brain characterized (e.g., medial temporal lobe only) and the classification of subjects/pathologies (e.g., clinical diagnoses only). Borthakur, et al.{20} examined the T1rho signal in the medial temporal lobe (MTL) gray and white matter in participants with Alzheimer's disease (AD) compared to mild cognitive impairment (MCI) and healthy controls (HC). On average, AD participants had a 6% increase in T1rho compared to controls (8% for WM and 5% for GM) with MCI participants having an intermediate mean value. The control and MCI participants tended to display a somewhat bimodal distribution in the WM T1rho values, assumed to be due to existing premorbid pathology in some subjects in these groups. Participant classification was based on neuropsychological tests, not knowledge of AD-specific pathologies. Although exhibiting positive change in T1rho in WM and GM with age, neither relationship was statistically significant. In the current investigation in which age was found to be a statistically significant factor, a 70 year old individual with cognitive impairment would exhibit global mean and median T1rho values that were 7.2% and 4.9% higher, respectively, than their healthy control counterparts, values consistent with the literature-reported differences.

Gray (GM) and white (WM) T1rho in the medial temporal lobe (MTL) in AD, MCI and age-matched controls were examined by Haris, et al.{22}. T1rho values were lowest in controls (87.5 ± 1.2 ms and 80.5 ± 1.4 ms), intermediate in MCI subjects (90.9 ± 1.3 ms and 84.1 ± 2.7 ms) and highest in AD patients (91.9 ± 0.8 ms and 88.3 ± 1.3 ms) in GM and WM, respectively. These differences were statistically significant between AD and controls but not between MCI and AD nor MCI and controls. No significant relationships between age and T1rho and MMSE and T1rho were observed. Five of the control subjects had significantly increased T1rho in both GM and WM.

Haris, et al.{21} examined the hippocampal (right (RH) and left (LH)) T1rho in controls and patients with Alzheimer's disease (AD) and Parkinson's disease without (PD) and with associated dementia (PDD). T1rho was significantly increased in AD compared to both controls and PD patients but not significantly different from PDD. PD patients were decreased compared to controls and PDD patients. Unlike in the current investigation, no significant correlations were observed between T1rho and age or T1rho and MMSE when limited to the hippocampal areas only. However, the authors concluded that serial T1rho imaging may provide insight into AD and PD disease progression and may assist in the early diagnosis of the diseases.

Haris, et al.{23} evaluated the sensitivity and specificity of the combination of T1rho of the WM and GM of the medial temporal lobe in combination with CSF biomarkers (β-amyloid$_{1-42}$, T-tau and P-tau 181p levels) for categorizing AD, MCI and controls who were classified based on a clinical consensus diagnoses. Using binary logistic regression, the combination of T1rho and CSF biomarkers predicted 86.4% of controls and 66.7% of MCI

subjects and 59.3% of MCI and 84.6% of AD subjects. Receiver operating characteristic (ROC) analyses found that T1rho exhibited greater sensitivity (control vs MCI: 0.60 vs 0.53; control vs AD: 0.82 vs 0.77 for T1rho and CSF biomarkers, respectively) and CSF biomarkers exhibited greater specificity (control vs MCI: 0.77 vs 0.82; control vs AD: 0.71 vs 0.79 for T1rho and CSF biomarkers, respectively) in distinguishing MCI and AD from controls. The investigators did not find any significant correlations between T1rho and CSF biomarkers or between T1rho and age. They concluded that the combination of T1rho and CSF biomarkers showed promise as a specific and early diagnostic for AD and may easily track the progression from MCI to AD.

In agreement with the literature, the current study found significant differences between the clinical diagnostic classifications and T1rho values (HC < cognitively impaired participants), however, by expanding the T1rho field-of-view (FOV) beyond the hippocampus and medial temporal lobe, the relationships between global T1rho and age and global T1rho and MMSE were discernable. In addition, a closer examination of Figure 2, highlights HC (green circles with red arrows) participants who may be potentially at enhanced risk of deterioration and MCI (blue diamonds with blue arrows) participants who may be at a lower risk of deterioration. Longitudinal follow-up would be needed to discern whether these differences translate to altered risk of deterioration. Analyses of regional T1rho values found significant relationships, only marginally with the medial temporal structures, but primarily with frontal, parietal, and cingulate structures, areas known to have AD-associated pathology (glucose hypometabolism, amyloid deposition).

T1rho MRI is a pH-sensitive measure with higher values consistent with a more acidic environment. The overall consistency of higher T1rho values with greater cognitive impairment and pathological burden is concordant with the development of acidosis as an integral component of the various AD-associated pathological cascades as described by Humpel.{1} By having a marker that varies according to a feature common to each of the cascades rather than one unique to a particular pathology only, it holds the possibility of placing an individual on a pathological trajectory rather than exhibiting a constellation of biomarker values for a particular level of impairment.{36} T1rho MRI holds promise as a potentially useful biomarker providing unique information beyond the T1-weighted measures of neurodegeneration.

However, there are limitations to the current study that warrant further investigation before the full utility of T1rho MRI can be determined. First, it should be noted that T1rho imaging is not exclusively sensitive to pH and other factors such as glucose{37} and glutamate{5} concentrations have been shown to influence T1rho relaxation times at higher magnetic fields and spin-lock amplitudes. In AD there are known changes in protein aggregates, glutamate and glucose concentrations that could influence T1rho relaxation times. Thus, it cannot be ruled out that other metabolites may be driving the T1rho relaxation time changes observed in this study. However, recent phantom work by Owusu, et al.{11} has found that the T1rho signal was more sensitive to changes in physiologic pH than to changes in glucose or lysine concentrations in a protein-rich medium (egg-white albumin phantom) at physiologic temperatures adding assurance that the observed *in vivo* T1rho signal likely reflects pH. Second, it is currently unknown if there are dispersion effects

of the spin-lock pulse *in vivo* that would vary its sensitivity across regions of the brain. Future studies may want to utilize several spin-lock amplitudes to evaluate dispersion effects and regional sensitivity. Third, the sample size in this study is small and skewed toward healthy controls with AD participants limited to the lower half of the age range only. A broader range of older participants with more extensive pathology will be needed to fully explore the interactions between age, cognitive impairment and pathological burden. Fourth, and most importantly, the current study is cross-sectional only. For T1rho MRI to be an effective metric of AD-associated pathology, it needs to be reproducible (i.e., produce the same values on day 1 compared to day 2), reliable (i.e., exhibit the same relationship between the T1rho measure, cognition and other pathological measures at time 1 and time 2), and longitudinally consistent (i.e., on an individual basis, increasing T1rho = decreasing cognitive performance; stable T1rho = stable cognition). Reproducibility data were not available for this subject population and scanner configuration. However, recent investigations using a state-of-the-art, high-resolution, efficient sagittal segmented 3D gradient echo sequence (TE=2.5ms; TR=5.6ms; field-of-view =220×220×160mm3; matrix = 128×128×80; flip angle = 10^{o}; and acceleration=2, spin-lock amplitude = 400Hz, spin-lock durations=0 and 80ms) implemented on a 3.0T GE Discovery 750W MRI Scanner indicates that for a limited group of subjects (N = 5) T1rho values were highly reproducible in the short term (i.e., 7 – 14 days) both regionally and globally. For a combination of subcortical and cortical hemispheric regions (N = 20/subject), the correlations between time 1 and time 2 were 0.90 and 0.92 with average differences of −1.7% and −1.1% for mean and median values, respectively. Data are currently not available to address the reliability and longitudinal consistency of these measures but are the basis of future T1rho-related research at this institution.

Conclusions

T1rho MRI, a pH-sensitive measure, was significantly associated with age and clinical status (healthy control versus cognitive impaired). After controlling for age, global T1rho MRI was positively associated with poorer cognition (lower MMSE) and memory (lower immediate and delayed memory scores); greater amyloid burden (based on [^{11}C]PIB SUVR and DVR), and more abnormal glucose metabolism. Regional T1rho MRI values in frontal and cingulate regions, after controlling for age, were positively associated with cognitive impairment. T1rho shows promise as a metric of AD-associated pathology potentially providing a single measure for assessing status and for monitoring the trajectory of the disease over time or with therapy.

Acknowledgments

This work was supported in part by the Biological Sciences Funding Program of the Office of the Vice President for Research, University of Iowa, Iowa City, Iowa and National Institutes of Health [R03AG047306 (Ponto, Schultz, co-PIs)]. The development of the T1rho imaging sequence was supported in part by National Institutes of Health [R01EB022019 and R01MH111578]. The MR imaging was performed on equipment supported by a high-end instrumentation grant [S10OD025025-01].

The content is solely the responsibility of the authors and does not necessarily represent the official views of the National Institutes of Health.

The authors would like to acknowledge Dr. Michael M. Graham, MD, PhD for allowing us to use [^{11}C]PIB under his physician-sponsored IND; Shannon Lehman, Karen Ekstam-Smith and Laura Temple for assistance in coordinating the research activities; Lea Weldon, RN and the technical staff of the PET Imaging Center.

References

1. Humpel C Chronic mild cerebrovascular dysfunction as a cause for Alzheimer's disease? Experimental Gerontology. 2011;46(4):225–32. [PubMed: 21112383]
2. Swerdlow RH. Mitochondria and Cell Bioenergetics: Increasingly Recognized Components and a Possible Etiologic Cause of Alzheimer's Disease. Antioxidants & Redox Signaling. 2012;16(12):1434–55. [PubMed: 21902597]
3. Mosconi L, Glodzik L, Mistur R, et al. Oxidative Stress and Amyloid-Beta Pathology in Normal Individuals with A Maternal History of Alzheimer's. Biological Psychiatry. 2010;68(10):913–21. [PubMed: 20817151]
4. Li PA, Siesjö BK. Role of hyperglycaemia-related acidosis in ischaemic brain damage. Acta Physiologica Scandinavica. 1997;161(4):567–80. [PubMed: 9429666]
5. Jin T, Kim S-G. Characterization of non-hemodynamic functional signal measured by spin-lock fMRI. NeuroImage. 2013;78:385–95. [PubMed: 23618601]
6. Kettunen MI, Gröhn OHJ, Silvennoinen MJ, et al. Effects of intracellular pH, blood, and tissue oxygen tension on T1ρ relaxation in rat brain. Magnetic Resonance in Medicine. 2002;48(3):470–7. [PubMed: 12210911]
7. Magnotta VA, Heo H-Y, Dlouhy BJ, et al. Detecting activity-evoked pH changes in human brain. Proceedings of the National Academy of Sciences. 2012;109(21):8270–3.
8. Jokivarsi KT, Hiltunen Y, Gröhn H, et al. Estimation of the Onset Time of Cerebral Ischemia Using T1ρ and T2 MRI in Rats. Stroke. 2010;41(10):2335–40. [PubMed: 20814006]
9. Mäkelä HI, Gröhn OHJ, Kettunen MI, et al. Proton Exchange as a Relaxation Mechanism for T1 in the Rotating Frame in Native and Immobilized Protein Solutions. Biochem Biophys Res Commun. 2001;289(4):813–8. [PubMed: 11735118]
10. Kettunen MI, Sierra A, Närväinen MJ, et al. Low Spin-Lock Field T1 Relaxation in the Rotating Frame as a Sensitive MR Imaging Marker for Gene Therapy Treatment Response in Rat Glioma. Radiology. 2007;243(3):796–803. [PubMed: 17517934]
11. Owusu N, Johnson CP, Kearney W, et al. R1ρ sensitivity to pH and other compounds at clinically accessible spin-lock fields in the presence of proteins. NMR in Biomedicine. 2019:e4217. [PubMed: 31742802]
12. Heo H-Y, Wemmie J, Thedens D, et al. Evaluation of activity-dependent functional pH and T1ρ response in the visual cortex. NeuroImage. 2014;95(0):336–43. [PubMed: 24486980]
13. Heo H-Y, Wemmie JA, Johnson CP, et al. Eccentricity mapping of the human visual cortex to evaluate temporal dynamics of functional T(1ρ) mapping. Journal of Cerebral Blood Flow & Metabolism 2015;35(7):1213–9. [PubMed: 25966957]
14. Johnson CP, Heo H-Y, Thedens DR, et al. Rapid acquisition strategy for functional T1ρ mapping of the brain. Magnetic Resonance Imaging. 2014;32(9):1067–77. [PubMed: 25093630]
15. Magnotta VA, Johnson CP, Follmer R, et al. Functional T1ρ Imaging in Panic Disorder. Biological Psychiatry. 2014;75(11):884–91. [PubMed: 24157339]
16. Johnson CP, Follmer RL, Oguz I, et al. Brain abnormalities in bipolar disorder detected by quantitative T1[rho] mapping. Mol Psychiatry. 2015;20(2):201–6. [PubMed: 25560762]
17. Johnson CP, Christensen GE, Fiedorowicz JG, et al. Alterations of the cerebellum and basal ganglia in bipolar disorder mood states detected by quantitative T1ρ mapping. Bipolar Disorders. 2018.
18. Wassef SN, Wemmie J, Johnson CP, et al. T1ρ imaging in premanifest Huntington disease reveals changes associated with disease progression. Movement Disorders. 2015;30(8):1107–14. [PubMed: 25820773]
19. Haris M, McArdle E, Fenty M, et al. Early marker for Alzheimer's disease: Hippocampus T1rho (T1ρ) estimation. Journal of Magnetic Resonance Imaging. 2009;29(5):1008–12. [PubMed: 19388096]

20. Borthakur A, Sochor M, Davatzikos C, et al. T1ρ MRI of Alzheimer's disease. NeuroImage. 2008;41(4):1199–205. [PubMed: 18479942]
21. Haris M, Singh A, Cai K, et al. T1rho (T1ρ) MR imaging in Alzheimer' disease and Parkinson's disease with and without dementia. Journal of Neurology. 2011;258(3):380–5. [PubMed: 20924593]
22. Haris M, Singh A, Cai K, et al. T1ρ MRI in Alzheimer's Disease: Detection of Pathological Changes in Medial Temporal Lobe. J Neuroimaging. 2011;21(2):e86–e90. [PubMed: 20331502]
23. Haris M, Yadav SK, Rizwan A, et al. T1rho MRI and CSF biomarkers in diagnosis of Alzheimer's disease. NeuroImage: Clinical. 2015;7:598–604. [PubMed: 25844314]
24. Mangia S, Svatkova A, Mascali D, et al. Multi-modal Brain MRI in Subjects with PD and iRBD. Frontiers in Neuroscience. 2017;11(709).
25. Nestrasil I, Michaeli S, Liimatainen T, et al. T1ρ and T2ρ MRI in the evaluation of Parkinson's disease. Journal of Neurology. 2010;257(6):964–8. [PubMed: 20058018]
26. Zhao F, Yuan J, Lu G, et al. T1ρ relaxation time in brain regions increases with ageing: an experimental MRI observation in rats. The British Journal of Radiology. 2016;89(1057):20140704. [PubMed: 26529226]
27. Menyhárt Á, Zölei-Szénási D, Puskás T, et al. Age or ischemia uncouples the blood flow response, tissue acidosis, and direct current potential signature of spreading depolarization in the rat brain. American Journal of Physiology-Heart and Circulatory Physiology. 2017;313(2):H328–H37. [PubMed: 28600353]
28. Watts R, Andrews T, Hipko S, et al. In vivo whole-brain T1-rho mapping across adulthood: Normative values and age dependence. Journal of Magnetic Resonance Imaging. 2014;40(2):376–82. [PubMed: 24227659]
29. Bonnet U, Bingmann D, Speckmann E-J, et al. Aging is associated with a mild acidification in neocortical human neurons in vitro. Journal of Neural Transmission. 2018;125(10):1495–501. [PubMed: 29995171]
30. Fang B, Wang D, Huang M, et al. Hypothesis on the Relationship Between the Change in Intracellular pH and Incidence of Sporadic Alzheimer's Disease or Vascular Dementia. International Journal of Neuroscience. 2010;120(9):591–5.
31. Petersen RC, Aisen PS, Beckett LA, et al. Alzheimer's Disease Neuroimaging Initiative (ADNI): clinical characterization. Neurology. 2010;74(3):201–9. [PubMed: 20042704]
32. Charagundla SR, Borthakur A, Leigh JS, et al. Artifacts in T1rho-weighted imaging: correction with a self-compensating spin-locking pulse. Journal of Magnetic Resonance. 2003;162(1):113–21. [PubMed: 12762988]
33. Price JC, Klunk WE, Lopresti BJ, et al. Kinetic modeling of amyloid binding in humans using PET imaging and Pittsburgh Compound-B. J Cereb Blood Flow Metab. 2005;25(11):1528–47. [PubMed: 15944649]
34. Lopresti BJ, Klunk WE, Mathis CA, et al. Simplified Quantification of Pittsburgh Compound B Amyloid Imaging PET Studies: A Comparative Analysis. J Nucl Med. 2005;46(12):1959–72. [PubMed: 16330558]
35. Benjamini Y, Hochberg Y. Controlling the false discovery rate: a practical and powerful approach to multiple testing. Journal of the Royal Statistical Society Series B (Methodological). 1995;57(1):289–300.
36. Jack CR Jr, Knopman DS, Jagust WJ, et al. Tracking pathophysiological processes in Alzheimer's disease: an updated hypothetical model of dynamic biomarkers. The Lancet Neurology. 2013;12(2):207–16. [PubMed: 23332364]
37. Jin T, Mehrens H, Hendrich KS, et al. Mapping Brain Glucose Uptake with Chemical Exchange-Sensitive Spin-Lock Magnetic Resonance Imaging. Journal of Cerebral Blood Flow & Metabolism. 2014;34(8):1402–10. [PubMed: 24865996]

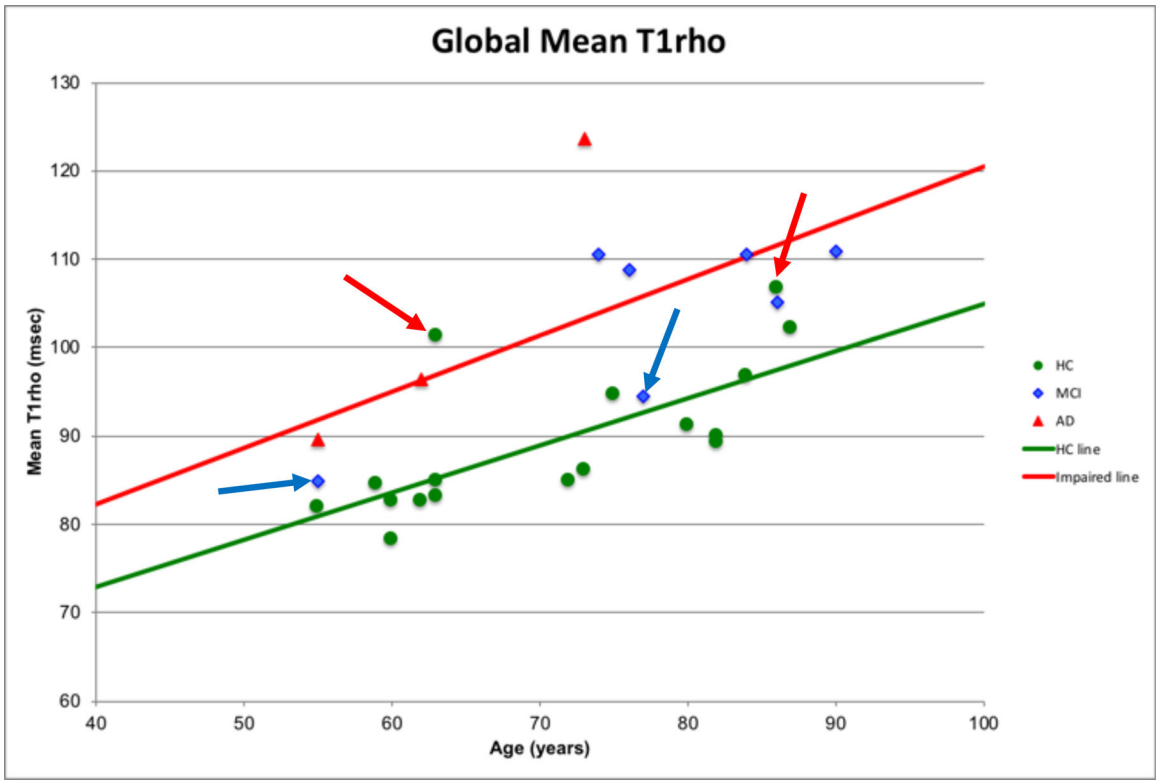

Figure 1.

The relationship between global mean T1rho (msec) and Age (years) by cognitive status. Normal cognition (healthy controls (HC)) (green line): Mean global T1rho = 51.6 + 0.53 × Age (R^2 = 0.51, p = 0.0014). Impaired cognition (MCI and AD): Mean global T1rho = 56.8 + 0.64 × Age (R^2 = 0.44, p = 0.036). Red arrows highlight HC participants with T1rho values more consistent with cognitive impairments and blue arrows highlight MCI participants with T1rho values more consistent with HCs.

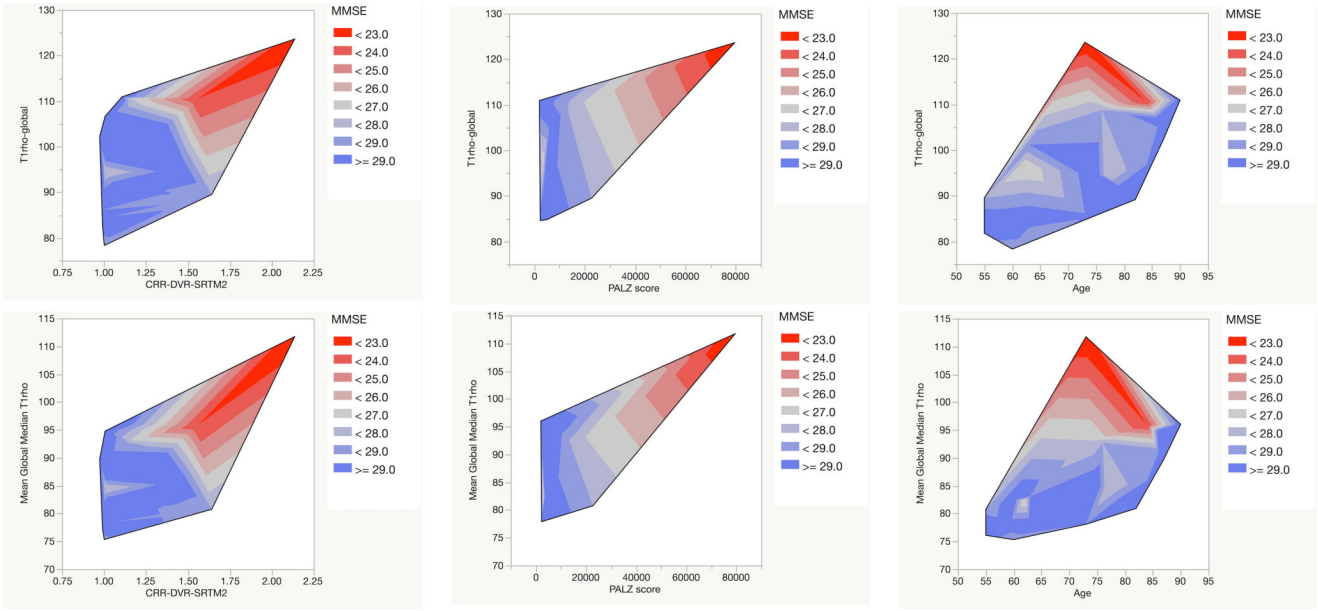

Figure 2.

Contour plots of T1rho – global (global volume-weighted mean of regional mean values) (upper row) and mean global median T1rho (global volume-weighted mean of regional median values) (lower row) versus amyloid burden (expressed as the cortical retention ratio calculated from the DVR) (left column), FDG-based Alzheimer's discrimination score (from PMOD PALZ) (middle column), and age (in years) contoured by Mini-Mental Status Exam score (MMSE) (red<gray<blue). Note the trend toward higher T1rho with lower MMSE (red) in all plots with corresponding higher amyloid burden (higher CRR) and more aberrant glucose metabolism (higher PALZ score) but not necessarily higher age.

Table 1.

Demographic, neuropsychological and global image-based parameters (Mean, Standard deviation (SD) and range)

	Healthy controls – cognitively normal (HC) (N = 17)			Cognitively Impaired (MCI and AD*) N = 10)			p-value**
Parameter	**Mean**	**SD**	**Range**	**Mean**	**SD**	**Range**	
Age (years	70.9	10.9	55 – 87	73.2	12.4	55 – 90	0.64
Sex	6 males, 11 females			7 males, 3 females			0.12
MMSE	29.6	0.6	28 – 30	27.0	2.7	22 – 30	0.15
Trail-making Test B-A (TMTB-A) (sec)	36.9	16.7	7 – 70	61.4	32.4	20 – 125	0.47
Logical Memory – Immediate (words)	14.6	3.0	7 – 19	8.1	3.8	3 – 15	0.0003
Logical Memory – Delayed (words)	14.1	2.6	8 – 19	5.0	2.9	0 – 8	<0.0001
PALZ PET Score	0.43	0.23	0.28 – 0.76	1.12	0.93	0.24 – 3.03	0.08
Cortical Retention Ratio (DVR)	1.1	0.1	1.0 – 1.5	1.4	0.4	1.0 – 2.1	0.05
Cortical Retention Ratio (SUVR)	1.2	0.2	1.1 – 1.8	1.5	0.4	1.1 – 2.5	0.05
Global Mean T1rho (sec)	89.5	8.2	78.3 – 106.7	103.5	11.9	84.8 – 123.6	0.005
Global Median T1rho (sec)	81.8	5.1	75.3 – 94.8	90.7	9.7	79.0 – 111.7	0.02
Cortical Volume (cc)	456	71	340 – 583	411	62	332 – 496	0.10

Definitions: MMSE = Mini-Mental Status Exam (scored 0 – 30), PALZ PET Score = FDG-based score derived by Alzheimer's Discrimination Tool (PALZ PMOD) with scores less than 1.0 considered to represent a normal FDG distribution and scores > 1.0 considered to represent an abnormal FDG distribution.

*AD participants were classified as having AD based on clinical diagnoses. One of the participants (62 year old, male) had compromised memory function (logical memory, delayed = 5 words) but only moderately impaired MMSE (26). His FDG scan was normal (PET score = 0.35) and a global mean T1rho = 96.5 and global median T1 rho = 82.3. He did not undergo amyloid imaging, so his clinical AD diagnosis is questionable.

**p-values: 2 sample t-test with Satterthwaite adjustment for unequal variance or Fisher's Exact Test.

Table 2.

Relationship Between T1rho Measures and Neuropsychological Testing and Imaging-based Parameters Controlling for Age (years)

Global Mean T1rho (seconds)					
Parameters	**Equation (T1rho = intercept + slope × Age + slope × parameter)**	**Direction**	**Parameter p value**	**R^2**	**Change in $R^2$with parameter**
Age only	= 49.3 + 0.63 Age	+	0.0008	0.37	
HC vs MCI_AD	= 54.8 + 0.58 Age − 6.4 [HC]	−	0.0002	0.65	0.28
MMSE	= 139.1 +0.60 Age − 3.0 MMSE	−	0.0001	0.66	0.29
Logical Memory – Immediate	=65.7 + 0.59 Age − 1.1 LMI	−	0.006	0.54	0.17
Logical Memory – Delayed	= 61.3 + 0.65 Age −1.3 LMD	−	<0.0001	0.68	0.31
TMTB-A	= 42.3 + 0.58 Age + 0.24 TMTB-A	+	0.0002	0.65	0.28
FDG PET Score (PALZ) (N = 12)	= 41.6 + 0.68 Age +10.3 PET	+	0.001	0.82	0.42 *
CRR (DVR)	= 22.5 +0.63 Age + 23.0 CRR (DVR)	+	0.0003	0.65	0.28
CRR (SUVR)	= 25.8 + 0.62 Age + 18.6 CRR (SUVR)	+	0.0005	0.65	0.28
Global Median T1rho (seconds)					
Parameters	**Equation (T1rho = intercept + slope × Age + slope × parameter)**	**Direction**	**Parameter p value**	**R^2**	**Change in $R^2$with parameter**
Age only	= 55.4 + 0.41 Age	+	0.002	0.32	
HC vs MCI_AD	= 58.9 + 0.38 Age − 4.0 [HC]	−	0.002	0.55	0.23
MMSE	= 122.5 +0.39 Age − 2.3 MMSE	−	<0.0001	0.65	0.33
Logical Memory – Immediate	= 65.9 + 0.38 Age − 0.69 LMI	−	0.018	0.47	0.15
Logical Memory – Delayed	= 63.1 + 0.43 Age −0.80 LMD	−	0.0009	0.58	0.26
TMTB-A	= 50.8 + 0.38 Age + 0.16 TMTB-A	+	0.001	0.57	0.25
FDG PET Score (PALZ) (N = 12)	= 44.6 + 0.50 Age + 9.0 PET	+	0.0002	0.87	0.52 *
CRR (DVR)	= 34.6 +0.39 Age + 19.1 CRR (DVR)	+	<0.0001	0.69	0.37
CRR (SUVR)	= 37.4 + 0.39 Age + 15.4 CRR (SUVR)	+	<0.0001	0.68	0.36

Definitions: HC = healthy control, MCI_AD = combined mild cognitive impairment and Alzheimer's disease participants, MMSE = MiniMental Status Exam, TMTB-A – Trailmaking test B minus Trailmaking Test A times (sec), FDG PET score (PALZ) = [^{18}F]fluorodeoxyglucose PET image score from the Alzheimer Discrimination Tool (PMOD), CRR = cortical retention ratio calculated from DVR = distribution volume ratio or SUVR = standardized uptake value ratio.

*Based participants with FDG imaging only (N = 12), Age only model had R^2 = 0.40 for global mean T1rho.

Table 3.

Relationship Between Regional T1rho Measures (median and mean) and Cognitive Status (healthy control (HC) versus mild cognitive impairment or Alzheimer's disease (MCI_AD)) Controlling for Age (years). Only regions for which both age and status were significant variables in the linear regression model are reported. Direction specifies the sign on the coefficient for the status variable (i.e., negative indicates that healthy controls have lower T1rho by the specified value). Bold values are significant after corrections for false discovery rate (FDR).

	Regional T1rho median				**Regional T1rho mean**			
Region	**Direction [HC]**	**p value**	**p value (FDR)**	**R^2**	**Direction [HC]**	**p value**	**p value (FDR)**	**R^2**
Frontal gyrus, inferior – left	-	**0.007**	**0.039**	**0.49**	-	0.016	0.10	0.58
Frontal gyrus, inferior – right	-	**0.002**	**0.031**	**0.59**	-	**0.0009**	**0.041**	**0.70**
Frontal gyrus, middle – left	-	**0.006**	**0.039**	**0.52**				
Frontal gyrus, middle – right	-	**<0.0001**	**<0.0001**	**0.74**	-	0.012	0.094	0.45
Frontal precentral gyrus – left	-	0.021	0.056	0.53				
Frontal precentral gyrus – right	-	0.012	0.051	0.62	-	0.019	0.11	0.66
Frontal gyrus, superior – right	-	0.047	0.099	0.65				
Cingulate gyrus, posterior – left	-	**0.0006**	**0.014**	**0.53**	-	0.0022	0.051	0.53
Cingulate gyrus, posterior – right	-	**0.0068**	**0.039**	**0.39**	-	0.022	0.11	0.41
Temporal gyrus, superior posterior – right	-	0.02	0.031	0.47				
Temporal lobe, posterior – right					-	0.0048	0.074	0.87
Insula, right	-	0.013	0.051	0.53	-	0.048	0.14	0.58
Parietal lobe, postcentral gyrus – left	-	**0.010**	**0.048**	**0.63**				
Parietal lobe, postcentral gyrus – right	-	0.017	0.053	0.61				
Parietal lobe, inferiolateral – left	-	**0.004**	**0.039**	**0.55**	-	0.036	0.12	0.57
Parietal lobe, inferiolateral – right	-	**0.0046**	**0.039**	**0.55**	-	0.0066	0.076	0.62
Parietal gyrus, superior – left	-	**0.010**	**0.048**	**0.48**				
Parietal gyrus, superior – right	-	0.045	0.099	0.49				
Thalamus – left	-	0.017	0.053	0.37	-	0.031	0.11	0.36
Thalamus – right	-	0.046	0.099	0.34	-	0.028	0.11	0.35
Corpus callosum					-	0.038	0.12	0.34
Caudate nucleus – left	-	0.05	0.10	0.33	-	0.024	0.11	0.44
Caudate nucleus – right					-	0.012	0.094	0.40